

SLAM-Free Visual Navigation with Hierarchical Vision-Language Perception and Coarse-to-Fine Semantic Topological Planning

Guoyang Zhao¹, Yudong Li², Weiqing Qi¹, Kai Zhang¹, Bonan Liu¹, Kai Chen¹, Haoang Li¹ and Jun Ma¹

Abstract— Conventional SLAM pipelines for legged robot navigation are fragile under rapid motion, calibration demands, and sensor drift, while offering limited semantic reasoning for task-driven exploration. To deal with these issues, we propose a vision-only, SLAM-free navigation framework that replaces dense geometry with semantic reasoning and lightweight topological representations. A hierarchical vision-language perception module fuses scene-level context with object-level cues for robust semantic inference. And a semantic-probabilistic topological map supports coarse-to-fine planning: LLM-based global reasoning for subgoal selection and vision-based local planning for obstacle avoidance. Integrated with reinforcement-learning locomotion controllers, the framework is deployable across diverse legged robot platforms. Experiments in simulation and real-world settings demonstrate consistent improvements in semantic accuracy, planning quality, and navigation success, while ablation studies further showcase the necessity of both hierarchical perception and fine local planning. This work introduces a new paradigm for SLAM-free, vision-language-driven navigation, shifting robotic exploration from geometry-centric mapping to semantics-driven decision making.

I. INTRODUCTION

Autonomous exploration and navigation remain fundamental challenges for mobile robots in open and unstructured environments. These capabilities are critical for applications such as search-and-rescue, warehouse logistics, and environmental monitoring, where robots must explore unknown areas, interpret scene semantics, and reach task-relevant targets [1]. Conventional navigation pipelines typically rely on Simultaneous Localization and Mapping (SLAM) with LiDAR or multi-sensor fusion for pose estimation and dense metric map construction [2]. However, such geometry-driven methods are brittle under the rapid motion and ground impacts of legged robots, where visual odometry often suffers from drift and tracking loss [3]. In addition, multi-sensor calibration and the high computational cost of dense mapping hinder deployment in lightweight, camera-only systems. For many task-driven applications, building dense maps is unnecessary; what is needed is a compact, scalable representation that supports efficient exploration.

Traditional SLAM-based navigation primarily focuses on geometric reconstruction and pose optimization, with limited support for semantic reasoning about the environment [4].

¹Guoyang Zhao, Weiqing Qi, Kai Zhang, Bonan Liu, Kai Chen, Haoang Li and Jun Ma are with the Robotics and Autonomous Systems Thrust, The Hong Kong University of Science and Technology (Guangzhou), China (email: {gzhao492, wqiaj, kzhang740, bliu404, kchen916}@connect.hkust-gz.edu.cn; haoangli@hkust-gz.edu.cn; jun.ma@ust.hk)

²Yudong Li is with the Department of Mechanical and Energy Engineering, Southern University of Science and Technology, China (email: 12432385@mail.sustech.edu.cn)

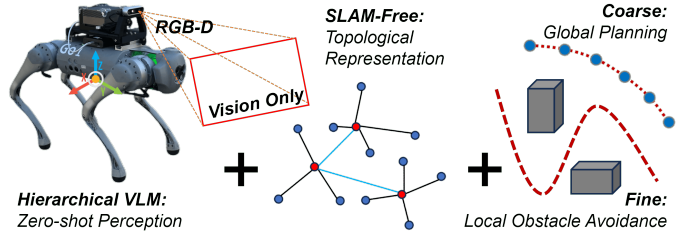


Fig. 1. SLAM-free semantic object exploration paradigm. The robot (left) processes RGB-D streams via a hierarchical perception module to construct a topological map (middle), where nodes denote semantic landmarks and edges represent paths. The robot then reaches the goal through a Coarse-to-Fine planning strategy (right).

This limitation is especially critical for open-set object search and semantic exploration tasks, where the robot must not only localize itself but also reason about which regions are worth exploring next, which objects are relevant to its mission, and how to plan under uncertainty. Compared with dense maps, topological representations are more compact and lightweight, while still capturing the essential connectivity of the environment and naturally supporting the integration of semantic labels for long-horizon exploration.

Recent advances in Vision-Language Models (VLMs) and Vision-Language Navigation (VLN) have opened new opportunities to endow robots with rich semantic understanding and language grounding [5]. These models can infer task-relevant object categories and scene descriptions from natural language instructions and visual inputs [6]. However, existing VLN approaches largely focus on perception and recognition, while overlooking the integration of global planning, decision-making, and fine-grained obstacle avoidance [7]. Furthermore, most prior works have been evaluated primarily in static or simulated environments and have not addressed the challenges of deploying such systems on real-world, heterogeneous legged platforms.

To address these challenges, we revisit the design of the robotic navigation stack from a system-level perspective and propose a purely visual, SLAM-free navigation framework (Fig. 1). Our framework relies exclusively on onboard cameras to achieve semantic-driven exploration and is designed with cross-platform deployability in mind. Specifically, we address four core challenges: (i) achieving robust perception and incremental exploration without explicit geometric SLAM; (ii) enabling robust semantic understanding in unstructured scenes; (iii) integrating global reasoning, local obstacle avoidance, and interpretable planning within a unified pipeline; and (iv) supporting rapid deployment and consistent performance across different types of legged robots.

To tackle these challenges, we propose a SLAM-Free vi-

sual navigation framework with hierarchical Vision-language perception and coarse-to-fine semantic topological planning, which integrates semantic perception, topological reasoning, and motion control into a unified architecture. Concretely, we design an adaptive hierarchical perception module that fuses scene-level and object-level outputs from VLMs to achieve robust semantic inference; construct a semantic-probabilistic topological map and perform coarse-to-fine planning via LLM-augmented global reasoning and vision-based local obstacle avoidance, replacing traditional geometry-based global path planning; and train reinforcement learning (RL)-based locomotion policies for different legged robot morphologies, enabling seamless integration and cross-platform deployment. Our main contributions are summarized as follows:

- 1) We present a purely visual, SLAM-free semantic exploration and navigation framework that addresses the fragility of SLAM on legged robots under rapid motion and sensor drift. The framework supports incremental target search in open-world environments while overcoming the limitations of geometry-centric approaches.
- 2) We design a hierarchical visual perception module with a lightweight adaptive fusion strategy that combines scene- and object-level VLM outputs for robust, context-aware understanding.
- 3) We construct a semantic-probabilistic topological map and propose a coarse-to-fine planning paradigm combining LLM-driven global reasoning with vision-based obstacle avoidance, serving as an alternative to SLAM.
- 4) We conduct comprehensive experiments in both simulation and real-world settings, showing gains in success rate, semantic accuracy, and path efficiency.

II. RELATED WORK

A. Semantic Understanding in Open-World Scenarios

Scene Level. Recent advancements in VLMs have significantly improved scene-level semantic understanding by integrating visual and textual modalities [8]. Models such as CLIP [9], Qwen-VL [10], MiniGPT-4 [11], and BLIP-2 [12] enable zero-shot recognition, image captioning, and visual question answering by aligning image and text embeddings through large-scale pretraining. These models are capable of providing holistic descriptions of open-world environments and generalizing across diverse scenes. However, their ability to precisely localize or distinguish specific targets remains limited. Most scene-level VLMs lack fine-grained spatial resolution and struggle with object-specific reasoning, making them insufficient for robotic interaction or navigation.

Object Level. To complement these limitations, object-level perception models such as Segment Anything Model (SAM) [13], Grounding DINO [14], YOLO-World [15], and OWL-ViT [16] have emerged. These models support promptable segmentation or open-vocabulary object detection, allowing for flexible and language-guided recognition of objects not seen during training. For instance, SAM produces segmentation masks for arbitrary object prompts, while Grounding DINO and YOLO-World enable text-guided object localization in complex scenes. Despite their

strong object-centric recognition ability, these models tend to lack contextual scene awareness. They typically treat detected objects in isolation and fail to encode broader spatial structures or relationships among objects and regions.

B. Robotic Exploration via Vision-Language Navigation

SLAM-based Exploration. SLAM has long been a cornerstone in autonomous robotic exploration, enabling robots to build and utilize maps of unknown environments. Traditional SLAM approaches, such as ORB-SLAM3 [3], offer robust visual-inertial localization and mapping capabilities. FAST-LIO [17] and its successor FAST-LIO2 [18] provide efficient LiDAR-inertial odometry solutions for real-time applications. [19] integrated deep reinforcement learning with robust SLAM to improve navigation in dynamic settings. In [20], a visual SLAM algorithm incorporating target detection and clustering to handle dynamic scenarios more effectively. However, SLAM-based methods often struggle with generalization to open-world environments and lack semantic understanding, limiting their applicability in complex, unstructured settings.

Vision-Language Navigation. VLN aims to guide robots through environments using natural language, integrating visual and linguistic information. In [21], the authors present VL-Nav, which combines pixel-wise vision-language features with heuristic exploration for real-time navigation. In [22], a volumetric environment representation is proposed to improve scene understanding. In [23], language as a perceptual representation is explored to boost performance in low-data settings. In [24], cross-modal map learning is introduced to link language with spatial representations. In [25], a dual-scale graph transformer is presented for joint long-term planning and fine-grained cross-modal reasoning. While these methods advance language–vision integration, they often lack the robust planning and obstacle avoidance needed for real-world deployment.

C. SLAM-Free Map Representation

Traditional SLAM-based methods rely on constructing dense geometric maps through feature matching, optimization, and loop closure [4], [26]. While effective in structured environments, these approaches incur high computational cost and struggle in dynamic or large-scale open-world scenarios, where maintaining a globally consistent metric map is expensive and brittle. Moreover, purely geometric maps lack semantic richness, limiting their utility for language-guided navigation and task-level reasoning.

To overcome these limitations, recent research has explored SLAM-free representations that replace dense geometry with lightweight, task-oriented maps. One class of approaches directly learns reactive navigation policies via reinforcement or imitation learning, bypassing explicit mapping altogether [27], [28]. Although efficient, these methods often suffer from limited interpretability and generalization. Another line of work leverages topological or graph-based representations, where nodes represent semantic landmarks and edges encode reachability or transition costs [29]. These

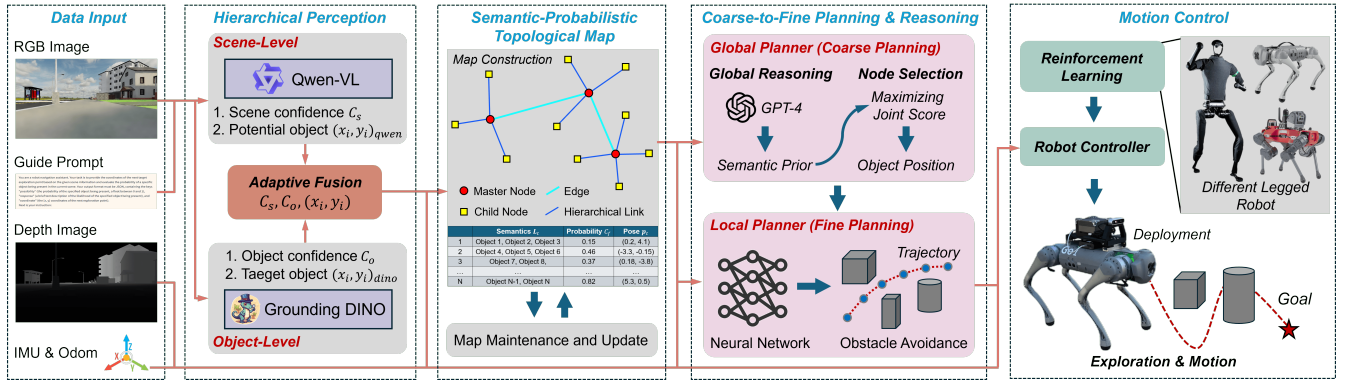


Fig. 2. Our SLAM-free vision-language navigation framework. The framework processes RGB-D input through hierarchical visual perception, constructs a semantic-probabilistic topological map, performs coarse global reasoning and fine local obstacle avoidance, and outputs control commands for robot locomotion, achieving goal-directed exploration without geometric SLAM.

approaches enable incremental exploration and are naturally compatible with semantic reasoning, making them well-suited for open-world tasks.

Building on this trend, we adopt a semantic-probabilistic topological map that not only stores node positions and semantic labels but also maintains confidence values for probabilistic reasoning. This representation supports dynamic updates as the robot explores new areas and allows global planning based on semantic relevance and accessibility.

III. METHODOLOGY

A. Framework Overview

Our framework provides a unified SLAM-free navigation pipeline that relies solely on onboard visual input and natural language instructions. As illustrated in Fig. 2, the system integrates hierarchical visual perception, semantic-probabilistic topological mapping, coarse-to-fine planning, and motion control. These modules are tightly coupled, transforming raw RGB-D observations into semantically grounded motion commands, thereby enabling robots to conduct robust goal-directed exploration without geometric SLAM.

At the start of each exploration episode, the robot performs a short initialization maneuver by rotating toward the four cardinal directions. Multi-view RGB-D images, together with odometry and IMU readings, are collected to seed the semantic-probabilistic topological map with a master node and its initial semantic proposals. This procedure ensures that the navigation process begins with both geometric coverage and semantic grounding, providing a reliable basis for subsequent perception, planning, and control.

B. Hierarchical Visual Perception

The hierarchical visual perception module employs a multi-stage process to extract robust semantic cues from RGB observations under natural language guidance. It consists of three components: scene-level interpretation, object-level detection, and an adaptive fusion strategy to generate reliable semantic targets for downstream topological mapping and planning.

1) **Scene-Level Interpretation:** For scene-level reasoning, we employ the Qwen2.5-VL-7B model [10] (accessed through its official API). The model aligns natural language instructions with RGB observations and outputs a global scene confidence score C_s together with a set of exploratory proposals $\mathbf{p}_i^{\text{qwen}} = (x_i, y_i)_{\text{qwen}}$ and corresponding semantic labels L_i . The confidence score C_s reflects the reliability of the global semantic interpretation, while $\mathbf{p}_i^{\text{qwen}}$ represents candidate exploration points.

2) **Object-Level Detection:** For object-level perception, we employ the GroundingDINO-T model with its official weights. The detector outputs an object confidence score C_o together with a set of proposals $\mathbf{p}_j^{\text{dino}} = (x_j, y_j)_{\text{dino}}$ and corresponding labels. The confidence score C_o quantifies the reliability of each detection, while $\mathbf{p}_j^{\text{dino}}$ provides accurate 2D localization of identified objects for subsequent semantic reasoning.

3) **Adaptive Fusion:** To integrate complementary cues from scene- and object-level perception, we adopt a lightweight Bayesian fusion scheme with geometric consistency weighting. For each candidate semantic target t observed by either module, we define its posterior score as:

$$S(t) \propto P(t) C_o^{\beta_o} C_s^{\beta_s} (\text{IoU}(\mathbf{p}_i^{\text{qwen}}, \mathbf{b}_j^{\text{dino}}) + \epsilon)^\lambda (\kappa(\mathbf{p}_i^{\text{qwen}}) + \epsilon)^\mu, \quad (1)$$

where $P(t)$ is a prior (set to 1 if no task-specific bias is available), $\beta_o, \beta_s \in [0.5, 2]$ weight the contribution of object and scene confidences, $\text{IoU} \in [0, 1]$ measures spatial overlap between the scene proposal region and object bounding box, and $\kappa \in [0, 1]$ is a coarse free-space indicator along the ray toward the candidate. Small constants $\epsilon \approx 10^{-3}$ ensures numerical stability, and exponents λ, μ control the impact of spatial and reachability consistency.

The final target selection is performed by normalizing all candidate scores and choosing the maximum:

$$t^* = \arg \max_t S(t), \quad C_f = \frac{S(t^*)}{\sum_t S(t)}. \quad (2)$$

If both scene- and object-level locations exist for t^* , the final 2D target is computed by reliability-weighted interpolation:

$$w = \frac{C_o^{\beta_o}}{C_o^{\beta_o} + C_s^{\beta_s}}, \quad \mathbf{p}_t = w \mathbf{p}_j^{\text{dino}} + (1 - w) \mathbf{p}_i^{\text{qwen}}, \quad (3)$$

otherwise, the single available point is used as \mathbf{p}_t .

The fused confidence C_f , selected target \mathbf{p}_t , and semantic label L_t are then forwarded to the Semantic-Probabilistic Topological Map module for incremental graph construction and global planning.

C. Semantic-Probabilistic Topological Map Representation

The semantic-probabilistic topological map serves as a lightweight representation of the explored environment, integrating spatial geometry, semantic context, and probabilistic cues to support downstream planning and reasoning. It incrementally grows as the robot explores and perceives new regions.

1) **Topological Map Definition and Structure:** We represent the environment as a graph $G = (V, E)$, where nodes $v_i \in V$ correspond to spatial locations and edges $e_{ij} \in E$ represent traversable connections weighted by traversal cost c_{ij} . Each node v_i stores its 3D position $\mathbf{P}_{v_i} = (X_{v_i}, Y_{v_i}, Z_{v_i})$, the semantic label L_{v_i} from the perception module, and a fused confidence score $C_{f_{v_i}}$. The robot's starting viewpoint is designated as the **master node** v_m . Newly observed locations from \mathbf{p}_t are back-projected into 3D world coordinates using depth and odometry measurements:

$$\mathbf{P}_{v_c} = \pi^{-1}(\mathbf{p}_t, D(\mathbf{p}_t)), \quad (4)$$

and are added as **child nodes** $v_c \in V$ if they exceed a spatial distance threshold from existing nodes.

2) **Semantic-Probabilistic Node Propagation:** Each node is associated with an exploration probability $P_{\text{explore}}(v_i)$, which reflects the likelihood that unexplored semantic content remains in that direction. The initial probability is set by fused confidence $C_{f_{v_i}}$ and is subsequently updated when the robot visits the node or observes new evidence. This update is modeled as a simple Bayesian belief revision:

$$P_{\text{explore}}^{\text{new}}(v_i) = \frac{P(\text{evidence}|v_i) P_{\text{explore}}^{\text{old}}(v_i)}{P(\text{evidence})}, \quad (5)$$

where $P(\text{evidence}|v_i)$ is derived from the observation of objects or regions around v_i . When the node is fully observed, its exploration probability is decayed toward zero, reducing its priority in future global planning.

3) **Map Maintenance and Update:** The topological graph is incrementally updated during exploration. When new nodes are added, edges are created to their k -nearest neighbors or those within a spatial threshold to preserve connectivity. Node attributes such as semantic labels and confidence scores are refreshed if stronger evidence becomes available. To prevent uncontrolled growth, nodes with confidence below a minimum threshold or exploration probability near zero are pruned. The resulting map maintains a compact, up-to-date representation of the environment, providing a semantic-rich but geometry-light basis for global reasoning and coarse-to-fine planning.

D. Coarse-to-Fine Planning & Reasoning

Building upon the semantic-probabilistic topological map, this module generates goal-directed navigation decisions by

combining global semantic reasoning with local obstacle-aware planning. We decompose the planning process into two complementary levels: a coarse global reasoning layer that selects the most promising exploration subgoal from the semantic topological graph, and a fine local planning layer that generates dynamically feasible trajectories to safely reach the chosen subgoal. This hierarchical structure serves as a substitute for traditional SLAM-based global planners and enables efficient and semantically meaningful exploration in previously unseen environments.

1) Coarse Planning of Global Topological Reasoning:

Given the current semantic-probabilistic topological graph $G = (V, E)$, we first collect all candidate child nodes $\{v_c\}$ whose exploration probability $P_{\text{explore}}(v_c)$ exceeds a minimum threshold. Each candidate node is described by its semantic label L_{v_c} , fused confidence $C_{f_{v_c}}$, and its estimated travel cost $d(\mathbf{P}_{\text{robot}}, \mathbf{P}_{v_c})$. To determine the next exploration target, we use a two-step approach:

(i) **LLM-based Semantic Reasoning.** We employ GPT-4 as a semantic reasoning engine to compute a relevance score $S_{v_c}^{\text{LLM}} \in [0, 1]$ for each candidate node. The model receives a compact prompt containing the task description, the set of semantic labels $\{L_{v_c}\}$, and the historical exploration context, and outputs a normalized score indicating the semantic importance of visiting each node. This allows the robot to incorporate high-level reasoning, such as prioritizing task-relevant objects or unexplored regions.

(ii) **Greedy Optimization.** After obtaining $S_{v_c}^{\text{LLM}}$, we select the next subgoal v^* by greedily maximizing a joint score that integrates semantic relevance, visual confidence, and reachability:

$$v^* = \arg \max_{v_c \in \{V\}_{\text{child}}} \left(S_{v_c}^{\text{LLM}} \cdot C_{f_{v_c}} \cdot \exp(-\gamma \cdot d(\mathbf{P}_{\text{robot}}, \mathbf{P}_{v_c})) \right), \quad (6)$$

where γ regulates the trade-off between semantic importance and spatial accessibility. This greedy strategy selects, at each step, the node that maximizes the expected exploration gain while minimizing travel cost, ensuring low computational complexity and real-time feasibility. The resulting subgoal node v^* and its 3D position \mathbf{P}_{v^*} are then passed to the fine planning layer for local trajectory generation.

2) **Fine Planning of Local Obstacle-Avoidance:** Given the subgoal \mathbf{P}_{v^*} , the fine planning layer computes a collision-free trajectory. We adopt *Viplanner* [1], an end-to-end vision-based local planner, which takes the current depth frame D_t and the 2D projection of the subgoal (x_{gt}, y_{gt}) as input and produces linear and angular velocity commands:

$$\begin{bmatrix} v_p \\ \omega_p \end{bmatrix} = f_{\text{viplanner}}(D_t, x_{gt}, y_{gt}), \quad (7)$$

where v_p and ω_p ensure collision-free motion toward the subgoal. These preliminary commands are further refined by the RL-based locomotion controller (Sec. III-E) to generate smooth and dynamically feasible joint-level actions. By combining LLM-guided global reasoning with geometry-aware local planning, this coarse-to-fine framework achieves incremental, semantically informed navigation without requiring

dense metric maps by SLAM, enabling robust goal-directed exploration in complex open-world environments.

E. Robot Locomotion & Control

To deploy the proposed navigation framework across heterogeneous legged platforms, we integrate reinforcement-learning-based locomotion policies with a lightweight controller interface. This allows the high-level planning and reasoning modules to remain agnostic to the robot morphology, while ensuring dynamically feasible and smooth execution of navigation commands.

1) **RL Locomotion:** We adopt RL policies to train low-level locomotion controllers for different robot morphologies, including quadruped and humanoid platforms. The RL policies are trained in simulation with domain randomization to improve transferability to the real world. Each policy outputs joint-level control commands or target velocities given the robot's proprioceptive state s_t and high-level velocity command $[v_p, \omega_p]^T$ from the local planner:

$$\mathbf{u}_t = \pi_\theta(s_t, v_p, \omega_p), \quad (8)$$

where π_θ is the learned locomotion policy parameterized by θ , and \mathbf{u}_t is the resulting motor torques or joint position targets. This design allows the same high-level navigation strategy to be deployed on different robots by simply swapping the trained policy, without retraining the planning stack.

2) **Controller Integration:** During navigation, preliminary commands $[v_p, \omega_p]^T$ generated by the fine planning layer in (7) are refined by the RL controller considering recent observation history \mathcal{H}_{t-1} and robot dynamics:

$$\mathbf{u}_t = f_{rl}(v_p, \omega_p, D_t, \mathcal{H}_{t-1}), \quad (9)$$

where D_t is the current depth frame, and \mathcal{H}_{t-1} encodes temporal context such as previous control inputs and contact states. The resulting control commands are smooth, dynamically consistent, and enable robust execution of obstacle-avoidance maneuvers on real hardware. This controller interface abstracts away platform-specific differences and ensures that the navigation framework remains modular and easily portable across robot types.

IV. EXPERIMENTS

A. Experimental Setup

Object-level detection is performed using GroundingDINO with its official checkpoint, executed locally with identical inference settings in both simulation and real-world experiments. GPT-4 and Qwen-VL are accessed through their official APIs. Simulation experiments are conducted on a workstation with an NVIDIA RTX4090 GPU. In real-robot experiments, the workstation performs GroundingDINO inference and API calls, while a Jetson AGX Orin manages planning and control. The two systems communicate over a wireless network via ROS to exchange subgoals, depth frames, and low-level commands in real time.

1) **Simulation Environment:** We use Isaac Sim and instantiate two types of environments: *CARLA Town1* (outdoor urban) and an *indoor warehouse*. Across these two environments we define in total five semantic exploration tasks. Each task is evaluated with 20 trials from randomized start poses (fixed random seeds per task for reproducibility). We also evaluate cross-morphology performance in simulation (e.g., quadruped and humanoid models) under the same task definitions and trial protocol.

2) **Real-World Environment:** We deploy the system on a Unitree Go1 quadruped equipped with a RealSense D435i RGB-D camera. We evaluate in five environments: an office (30 m^2) with randomly placed desks/chairs/cabinets; a showroom (40 m^2) with display boards and machines; a laboratory (30 m^2) with manually constructed obstacle courses; a living room (30 m^2) with household objects; and an outdoor garden (50 m^2) with grass and tree obstacles. RGB-D streams are recorded at 30 FPS; pose/odometry is taken from the Go1 internal estimator. Each real-world task is executed for 20 trials from randomized start poses under identical instructions and time budgets.

3) **Evaluation Metrics:** We evaluate our navigation framework along two dimensions: perception and planning, and overall navigation.

(i) **Perception and Planning.** Semantic perception is measured by *Semantic Accuracy (SA)*, defined as $\text{SA} = \frac{1}{N} \sum_{i=1}^N \mathbb{I}[\text{reached_category}_i = \text{instructed_category}_i]$. Global planning is evaluated by *Global Node Selection Accuracy (GNSA)*,

$$\text{GNSA} = \frac{1}{\sum_{i=1}^N T_i} \sum_{i=1}^N \sum_{t=1}^{T_i} \mathbb{I}[v_{i,t}^* = v_{i,t}^{\text{oracle}}], \quad (10)$$

which measures node-selection correctness against the oracle path. Local safety is quantified by the *Obstacle Avoidance Success Rate (OASR)*, defined as

$$\text{OASR} = 1 - \frac{1}{N} \sum_{i=1}^N \mathbb{I}[\text{collision in trial } i], \quad (11)$$

where a collision is detected when the robot breaches the clearance threshold. This metric directly reflects the proportion of trials completed without collision, making it intuitive for evaluating local planning robustness.

(ii) **Overall Navigation.** Navigation performance is measured by *Success Rate (SR)* and *Success weighted by Path Length (SPL)*. Formally, $\text{SR} = \frac{1}{N} \sum_{i=1}^N \mathbb{I}[\|\mathbf{P}_i - \mathbf{G}_i\|_2 < r_s]$, where \mathbf{P}_i and \mathbf{G}_i denote the final and goal positions, respectively. SPL is defined as $\text{SPL} = \frac{1}{N} \sum_{i=1}^N S_i \cdot \frac{L_i^*}{\max(L_i, L_i^*)}$, where L_i and L_i^* are the executed and geodesic path lengths, and S_i is a binary success flag. All results are reported as mean \pm standard deviation over 20 trials.

B. Perception Fusion Experiments

We evaluate the proposed hierarchical visual perception module in simulation, using SA as the primary metric during autonomous exploration. At each exploration step,

TABLE I
SEMANTIC ACCURACY (%) ACROSS PERCEPTION STRATEGIES.

No.	Scene	Object	Scene	Weight Fusion	Adaptive Fusion
1	Garden	86.1	84.0	87.4	88.3
2	Sidewalk	87.0	85.1	88.7	89.3
3	Road	89.3	88.2	89.8	90.1
4	Warehouse (a)	87.7	85.6	87.4	88.6
5	Warehouse (b)	85.5	83.8	86.2	87.8

TABLE II
COARSE-TO-FINE PLANNING RESULTS.

No.	Scene	GNSA (%)			OASR (%)
		Probability	LLM	LLM + Opt.	
1	Garden	76.8	81.7	83.5	79.3
2	Sidewalk	78.1	83.3	85.0	80.9
3	Road	79.5	84.6	86.8	84.2
4	Warehouse (a)	78.9	84.0	86.2	82.7
5	Warehouse (b)	76.2	81.4	83.1	79.5

the robot captures RGB images at selected viewpoints, and predicted semantic categories are compared against ground-truth annotations across five representative scenes, including outdoor (garden, sidewalk, road) and indoor (two warehouse layouts) environments with diverse open-set objects.

Table I reports the SA under four settings: (i) *Scene-level only* using Qwen-VL for global scene interpretation, (ii) *Object-level only* using Grounding DINO for open-vocabulary detection, (iii) *Naive Weight Fusion* with fixed 1:1 averaging of both outputs, and (iv) *Adaptive Fusion*, our proposed Bayesian fusion with confidence- and geometry-based weighting.

Object-level perception consistently outperforms scene-level interpretation, with an average gain of +1.78% across all environments, highlighting the benefit of precise object localization. Simple weight fusion further improves accuracy to 87.9%, suggesting complementarity between scene-level context and object-level cues. Our adaptive fusion achieves the highest overall performance, reaching an average SA of 88.8%, providing +0.9% absolute improvement over naive fusion and +1.7% over object-only perception. These results prove that dynamically weighting scene- and object-level evidence yields more robust and context-aware semantic reasoning, leading to more reliable target proposals for subsequent topological mapping and planning.

C. Planning and Reasoning Experiments

We evaluate the proposed coarse-to-fine planning framework on both global topological reasoning and local obstacle-aware planning under autonomous exploration.

1) **Coarse Global Reasoning:** We compare three strategies for selecting exploration nodes from the semantic-probabilistic topological map: (i) *Probability-Only*, ranking nodes by raw semantic confidence; (ii) *LLM*, using GPT-4 for context-aware reasoning; and (iii) *LLM+Opt.*, which further incorporates traversal cost via (6).

As shown in Table II, LLM reasoning improves node

TABLE III
NAVIGATION RESULTS IN SIMULATION (20 TRIALS PER SCENE).

No.	Scene	Goal	SR (%)	SPL (%)
1	Garden	Green Bin	55	33.6
2	Sidewalk	Traffic Sign	60	40.5
3	Road	Bus Station	75	46.3
4	Warehouse (a)	Loading Cart	65	42.2
5	Warehouse (b)	Extinguisher	50	29.7

TABLE IV
NAVIGATION RESULTS IN REAL WORLD (20 TRIALS PER SCENE).

No.	Scene	Goal	SR (%)	SPL (%)
1	Office	Extinguisher	45	27.9
2	Showroom	Quadruped Robot	50	32.6
3	Laboratory	Black Chair	45	31.1
4	Living Room	Bucket Shelf	30	21.4
5	Garden	Carton Box	35	24.8

selection accuracy by an average of +5.1% over probability-only ranking, and the cost-aware optimization adds another +1.9%. These results confirm that semantic reasoning and spatial cost consideration are complementary, enabling more efficient exploration with fewer redundant visits.

2) **Fine Local Planning:** Local planning performance is assessed by the OASR, i.e., the proportion of trials completed without collisions. Our planner achieves an average of 81.3%, with Scene 4 reaching 84.2% due to improved handling of narrow passages.

Overall, accurate global subgoal selection and robust local planning form a coherent coarse-to-fine pipeline, supporting safe and efficient navigation without dense metric maps.

D. Comprehensive Navigation Experiments

1) **Simulation Experiments:** We first evaluate our framework in simulation using five representative scenes (Fig. 3) that cover both outdoor (garden, sidewalk, road) and indoor (two warehouse layouts) settings.

Table III summarizes the results. The framework achieves its highest SR in the *road* scenario (75%) with an SPL of 46.3%, benefiting from relatively open geometry and high-visibility targets. Performance decreases in more cluttered warehouse scenes, where occlusion and narrow passages occasionally cause perception or planning failures, resulting in lower SR (down to 50%) and reduced SPL (29.7%). Overall, the results demonstrate that our system can successfully complete semantic exploration tasks in diverse simulated environments, with SPL values indicating that the executed paths remain reasonably close to geodesic shortest paths.

2) **Real-World Experiments:** We further deploy our system on a Unitree Go1 quadruped and conduct experiments in five real-world environments: office, showroom, laboratory, living room, and outdoor garden. Fig. 4 shows typical robot trajectories and the corresponding semantic-probabilistic maps. The graphs indicate that the robot incrementally expands its semantic knowledge and converges to the correct target node when perception succeeds.

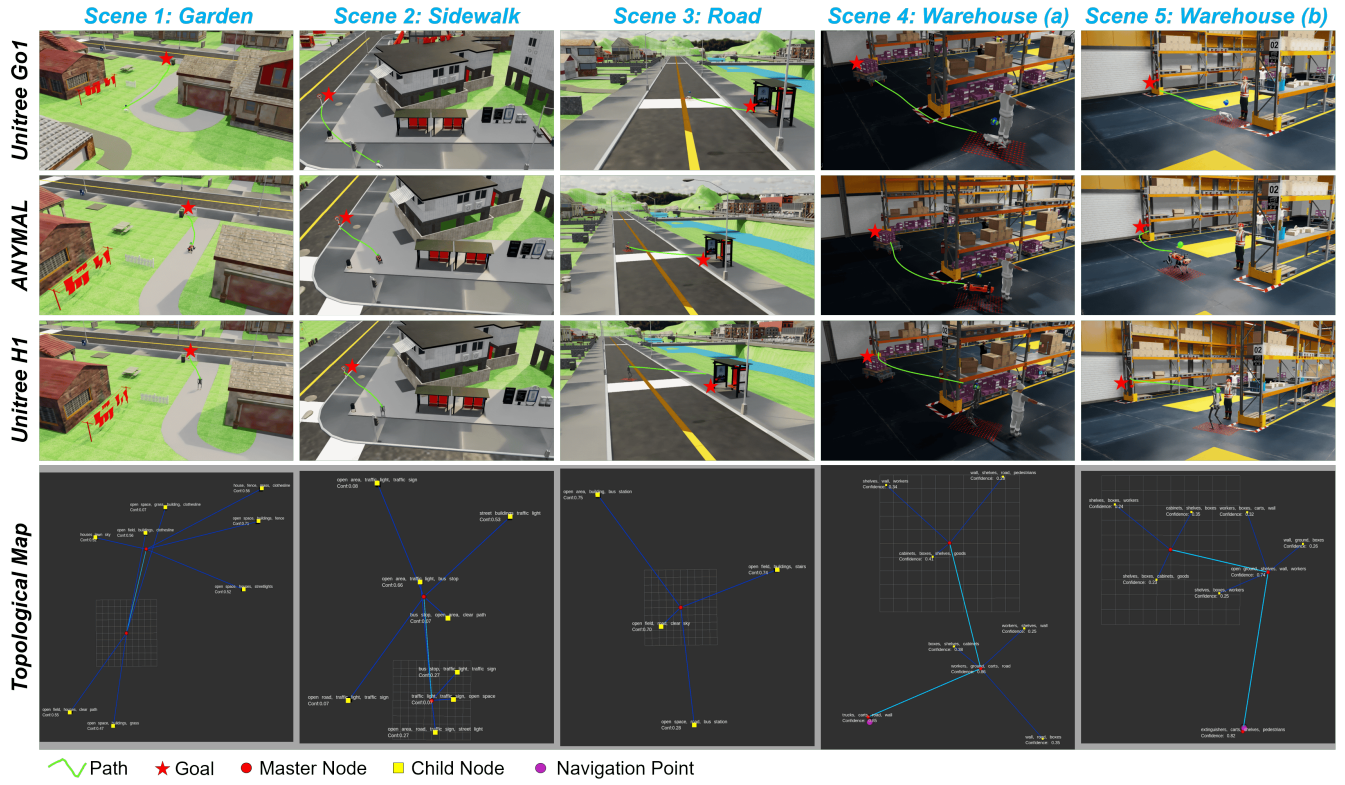


Fig. 3. **Simulation results across five environments with multiple robot morphologies.** We evaluate our SLAM-free navigation framework in *Garden*, *Sidewalk*, *Road*, and two *Warehouse* scenarios. Experiments are conducted using three different legged robot platforms, Unitree Go1, ANYmal, and Unitree H1, demonstrating the robustness and cross-platform adaptability.

The quantitative results are summarized in Table IV. Performance generally decreases compared to simulation due to real-world perception noise, motion blur, and challenging illumination. The highest performance is observed in the showroom scene (SR 50% and SPL 32.6%), which features wide corridors and clear visibility of the quadruped robot target. The most challenging environment is the living room, where heavy clutter and occlusions lead to the lowest SR (30%) and SPL (21.4%).

E. Ablation Studies

We conduct an ablation study to quantify the contribution of the hierarchical perception and coarse-to-fine planning modules. As shown in Table V, removing the object-level model and using only scene-level VLM significantly reduces navigation performance (SR 35% and SPL 19.5%), confirming that single-source perception is vulnerable to clutter and viewpoint changes. Combining scene- and object-level cues improves SR by +10% and SPL by +7.3%, demonstrating that complementary global context and localized object evidence are crucial for robust semantic target detection.

Similarly, incorporating the fine local planner on top of coarse global reasoning yields a further +10% SR gain and improves SPL to 30.2%, highlighting its role in safe traversal and path efficiency. These results validate that both hierarchical perception and coarse-to-fine planning are indispensable for reliable SLAM-free semantic navigation.

TABLE V
ABLATION EXPERIMENTS OF DIFFERENT MODULES.

Scene	Object	Hierarchical Perception		Coarse-to-Fine Planning	SR (%)	SPL (%)
		Global	Local			
✓			✓		35	19.5
✓	✓	✓	✓		45	26.8
✓	✓	✓	✓	✓	55	30.2

V. DISCUSSION

This work presents a first attempt toward SLAM-free semantic navigation using purely visual inputs, aiming to validate the feasibility of an open-world, SLAM-free exploration framework. Our experiments are therefore designed primarily around ablations and module-level analysis within the framework itself, rather than direct comparisons to SLAM-based or VLN baselines. While this choice clarifies the contribution of each component, it also limits the breadth of evaluation. The current validation further covers only a modest set of environments and robot platforms. Future work will expand toward standardized benchmarks for SLAM-free semantic exploration, incorporate temporal and uncertainty-aware reasoning to improve robustness, and extend evaluation to dynamic, large-scale real-world scenarios.

VI. CONCLUSION

We present a purely visual, SLAM-free navigation framework that integrates hierarchical vision–language perception, a semantic–probabilistic topological map, and a coarse-to-fine planning strategy with RL-based locomotion. The

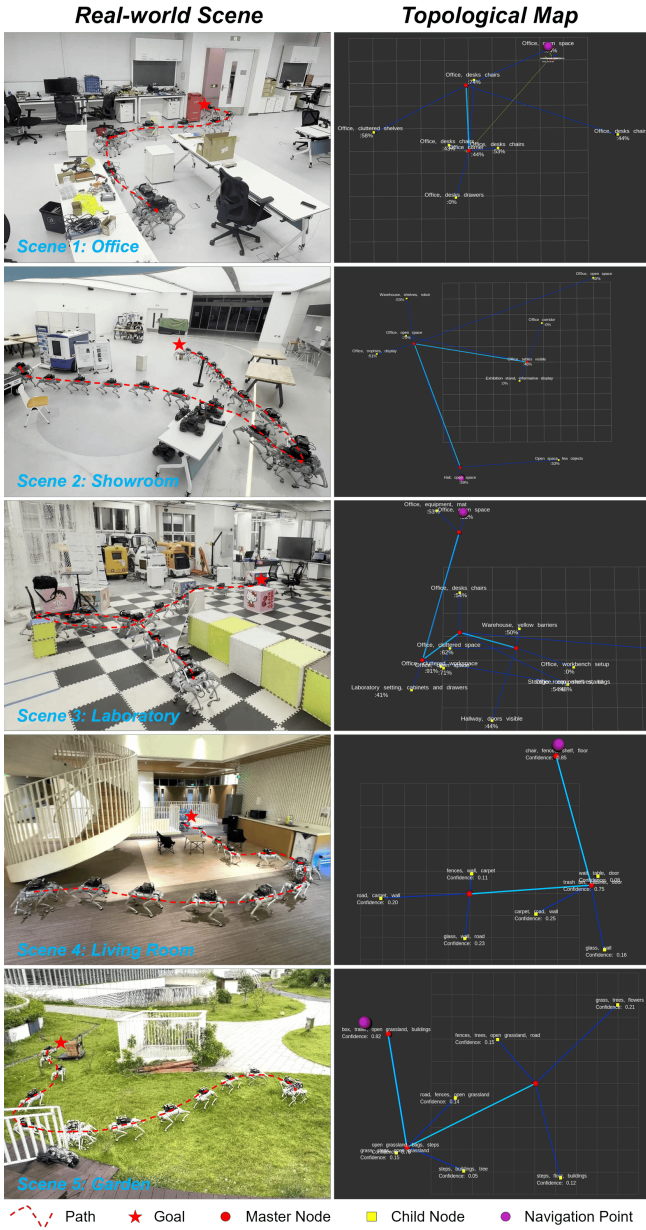


Fig. 4. **Real-world results across five environments.** Exploration trajectories and semantic-probabilistic topological maps are shown for Office, Showroom, Laboratory, Living Room, and Garden using Unitree Go1.

system demonstrates that compact semantic topology, rather than dense metric mapping, is sufficient for reliable goal-directed exploration. By unifying adaptive perception, global reasoning, and local obstacle-aware planning, our framework provides a lightweight yet robust solution for semantic navigation in open-world environments. This work lays the foundation for future SLAM-free benchmarks and scalable deployment across diverse robotic platforms.

REFERENCES

Figure 4 displays real-world results across five environments: Office, Showroom, Laboratory, Living Room, and Garden. Each environment is shown in a 'Real-world Scene' image and a corresponding 'Topological Map'. The maps are semantic-probabilistic graphs where nodes represent entities and edges represent confidence levels. The legend indicates: Path (red dashed line), Goal (red star), Master Node (red circle), Child Node (yellow square), and Navigation Point (purple circle).

Figure 4. Real-world results across five environments. Exploration trajectories and semantic-probabilistic topological maps are shown for Office, Showroom, Laboratory, Living Room, and Garden using Unitree Go1.

system demonstrates that compact semantic topology, rather than dense metric mapping, is sufficient for reliable goal-directed exploration. By unifying adaptive perception, global reasoning, and local obstacle-aware planning, our framework provides a lightweight yet robust solution for semantic navigation in open-world environments. This work lays the foundation for future SLAM-free benchmarks and scalable deployment across diverse robotic platforms.

- [26] R. Mur-Artal, J. M. M. Montiel, and J. D. Tardós, “ORB-SLAM: A versatile and accurate monocular SLAM system,” *IEEE Transactions on Robotics*, vol. 31, no. 5, pp. 1147–1163, 2015.
- [27] Y. Zhu, R. Mottaghi, E. Kolve, J. J. Lim, A. Gupta, L. Fei-Fei, and A. Farhadi, “Target-driven visual navigation in indoor scenes using deep reinforcement learning,” in *2017 IEEE international conference on robotics and automation*. IEEE, 2017, pp. 3357–3364.
- [28] M. Pfeiffer, S. Shukla, M. Turchetta, C. Cadena, A. Krause, R. Siegwart, and J. Nieto, “Reinforced imitation: Sample efficient deep reinforcement learning for mapless navigation by leveraging prior demonstrations,” *IEEE Robotics and Automation Letters*, vol. 3, no. 4, pp. 4423–4430, 2018.
- [29] D. S. Chaplot, R. Salakhutdinov, A. Gupta, and S. Gupta, “Neural topological SLAM for visual navigation,” in *Proceedings of the IEEE/CVF Conference on Computer Vision and Pattern Recognition*, 2020, pp. 12 875–12 884.